Journal of Power Sources 196 (2011) 159–163

Contents lists available at ScienceDirect

Journal of Power Sources

journal homepage: www.elsevier.com/locate/jpowsour

Short communication

Effect of electrode fabrication methods on the electrode performance for ethanol oxidation

Yuan-Hang Qin[a], Hui-Cheng Li[a], Hou-Hua Yang[a], Xin-Sheng Zhang[a,*], Xing-Gui Zhou[a], Li Niu[b], Wei-Kang Yuan[a]

[a] State Key Laboratory of Chemical Engineering, East China University of Science and Technology, Shanghai 200237, China
[b] State Key Laboratory of Electroanalytical Chemistry, Chang Chun Institute of Applied Chemistry, Chinese Academy of Sciences, Changchun 130022, China

ARTICLE INFO

Article history:
Received 26 May 2010
Received in revised form 13 June 2010
Accepted 15 June 2010
Available online 23 June 2010

Keywords:
Carbon nanofiber
Palladium
Ethanol oxidation
Electrophoretic deposition
Pulse electrodeposition
Electrode fabrication

ABSTRACT

Two palladium/carbon nanofibers modified glassy carbon electrodes, Pd/CNFs/GC-C and Pd/CNFs/GC-E, are fabricated by the conventional powder type method and by the electrophoretic deposition in conjunction with pulse electrodeposition method, respectively. Field emission scanning electron microscopy and high resolution transmission electron microscopy reveal that Pd particles are uniformly dispersed on the two electrodes and X-ray diffraction shows the average Pd particle size of the Pd/CNFs/GC-E electrode is slightly larger than that of the Pd/CNFs/GC-C electrode. Cyclic voltammetric analysis shows that the electrocatalytic activity of Pd/CNFs/GC-E electrode is better than that of Pd/CNFs/GC-C electrode for ethanol oxidation in alkaline media, although the latter has higher Pd loading than the former. This is believed to be due to the higher utilization of Pd catalyst on Pd/CNFs/GC-E electrode than on Pd/CNFs/GC-C electrode, which is confirmed by the electrochemically active surface area measurements. In addition, chronopotentiometric analysis shows the long-term operation stability of Pd/CNFs/GC-E electrode is better than that of Pd/CNFs/GC-C electrode.

1. Introduction

Recently, direct ethanol fuel cells (DEFCs) have drawn increasing attention because ethanol is less toxic compared to methanol and can be easily produced in large quantity from fermentation of biomass [1–3]. However, even when the expensive Pt-based electrocatalysts are used, the oxidation kinetics of ethanol in acidic media is still very sluggish, which limits the performance of DEFCs. It is therefore of much interest to develop high efficient electrocatalysts for ethanol oxidation reaction (EOR) by suitable ways. One way to achieve this goal is by operating DEFCs in alkaline environment, where the less expensive Pd-based electrocatalysts have electrocatalytic activities comparable to, or even better than Pt-based ones for ethanol oxidation [4,5]. Another way to achieve this goal is by employing high surface area supports and suitable electrode fabrication methods to improve the utilization of catalyst [6].

As novel carbon materials, carbon nanofibers (CNFs) offer an ideal opportunity as catalyst support due to their superior electronic conductivity, anti-corrosion ability, and high surface area [7]. There are many investigations which show that the electrocatalysts supported on CNFs possess enhanced catalytic activities [8–9].

Methods for fabricating electrodes can be roughly divided into two main types—powder and non-powder type. In the case of powder type method, the common procedure for fabricating an electrode is to mix the noble metal/support agglomerates with a polymer binder (such as Nafion) and apply this past to a substrate such as carbon cloth or carbon paper. It is claimed that the utilization of the noble metal catalysts is very low because there is a significant portion of noble metal catalyst that is isolated from reactants or external circuits on the electrodes fabricated by powder type methods [6,10–12]. Several non-powder type electrode fabrication methods, which create catalysts directly on the surface of carbon electrodes or membranes by using electrodeposition technique, were developed with the aim to improve the utilization of noble metal catalysts [6,10,13]. However, the effect of electrode fabrication methods on the electrode performance has not been experimentally investigated. In this work, a glassy carbon (GC) electrode was employed as a substrate, and a novel type of Pd/CNFs modified GC electrode, designated as Pd/CNFs/GC-E, was fabricated by using electrophoretic deposition (EPD) in conjunction with pulse electrodeposition (PED) method. For comparison, a conventional powder type method was employed to fabricate the powder type Pd/CNFs modified GC electrode, which was designated as Pd/CNFs/GC-C. The performance of the two electrodes for ethanol oxidation in KOH solution was compared.

* Corresponding author. Tel.: +86 21 64253469; fax: +86 21 64253528.
E-mail address: xszhang@ecust.edu.cn (X.-S. Zhang).

0378-7753/$ – see front matter © 2010 Elsevier B.V. All rights reserved.
doi:10.1016/j.jpowsour.2010.06.057

2. Experimental

2.1. Synthesis and functionalization of CNFs

Platelet type CNFs were synthesized and purified according to the literature [14–15]. The surface functionalization of CNFs was realized by sonochemical treatment [16]. Briefly, 250 mg of the CNFs was sonochemically treated in a solution containing 188 ml con. HNO_3, 160 ml con. H_2SO_4 and 12 ml de-ionized H_2O for 2 h at 65 °C. After surface treatment, the CNFs were rinsed thoroughly with de-ionized water until neutral, dried overnight at 120 °C and then stored in a sealed vessel for use.

2.2. Fabrication of catalyst electrodes

The Pd/CNFs/GC-C electrode was fabricated according to the literature [17]. Typically, 10 wt% Pd/CNFs were prepared by dissolving the required amount of $PdCl_2{\cdot}2H_2O$ and CNFs in HCl-acidified double distilled water. Subsequently, an excessive $NaBH_4$ solution was dropped into the above solution in a drop-wise manner under vigorous stirring. The resulted material was washed with double distilled water and dried at 40 °C at vacuum. To obtain the Pd/CNFs/GC-C electrode, the Pd/CNFs powder was dispersed ultrasonically in a 0.5% Nafion solution to obtain a homogeneous ink with a concentration of ca. 5 mg ml^{-1}, and 10 μl of the ink was pipette onto the surface of a GC electrode (3 mm in diameter). The Pd/CNFs/GC-C electrode was dried at room temperature in ambient air for 2 h and washed with double distilled water before use.

The Pd/CNFs/GC-E electrode was fabricated by using EPD in conjunction with PED method. (1) EPD process: 30 mg of CNFs were dispersed in 100 ml of absolute ethanol by ultrasonication, and 3 mg of $Mg(NO_3)_2{\cdot}6H_2O$ was added into the suspension to charge the CNFs which were negatively charged due to the oxygen-containing functional groups generated by the surface treatment. The above suspension, with positively charged CNFs due to the adsorbed Mg^{2+}, was employed as electrolyte for EPD. A GC electrode (3 mm in diameter) and an iridium oxide-coated titanium mesh were used as cathode and anode, respectively, and a dc voltage of 30 V lasted for 8 min was applied on the EPD electrodes with an electrode separation distance of 1 cm. During the EPD process, the positively charged CNFs were electrophoretically deposited onto the GC electrode. After EPD, the CNFs modified GC electrode (CNFs/GC) was dried at 120 °C for 2 h and then placed in ambient air for use in the deposition of Pd particles. (2) PED process: PED was performed on the CNFs/GC electrode using a Pd plating bathing containing 0.01 M $PdCl_2{\cdot}2H_2O$ solution with a pH value of 1.5 adjusted by HCl solution, and the CNFs/GC electrode was used as cathode and a Pt foil as anode. A PGSTAT 30 electrochemical workstation (Eco Chemie B.V. Netherlands) was employed as controller of the electrochemical parameters, which were: peak current density = 50 mA cm^{-2}, on time = 100 ms, off time = 700 ms and applied charge = 0.140 C cm^{-2}. The obtained Pd/CNFs/GC-E electrode was dried at 120 °C in ambient air for 2 h and washed with double distilled water before use.

2.3. Characterization of electrodes

X-ray diffraction (XRD) patterns of the Pd/CNFs catalysts were recorded on an X-ray diffractometer (D/MAX 2550 VB/PC, RIGAKU) at a sweep rate of 2° min^{-1} using Cu Ka as radiation source (λ = 0.154056 nm). The CNF loadings determined by UV–vis spectroscopy (Varian Cary 500) [18] were 606 and 613 μg cm^{-2} on Pd/CNFs/GC-E and Pd/CNFs/GC-C electrode, respectively. The Pd loadings determined by inductively coupled plasma atomic emission spectrometry (ICP-AES, Thermo Elemental IRIS 1000) were 55.7 and 64.4 μg cm^{-2} on the Pd/CNFs/GC-E and Pd/CNFs/GC-C electrode, respectively. Field emission scanning electron microscopy (FESEM FEI Quanta 400 FEG) was employed to characterize the morphology of CNFs supported Pd particles. High resolution transmission electron microscopy (HRTEM FEI Tecnai G2 F30 S-Twin) was used in the Pd particle size and size distribution analysis. Electrochemical measurements were carried out on the PGSTAT 30 electrochemical workstation. All experiments were conducted in a conventional three-electrode system with a Pt foil counter electrode and a saturated calomel electrode (SCE) reference electrode.

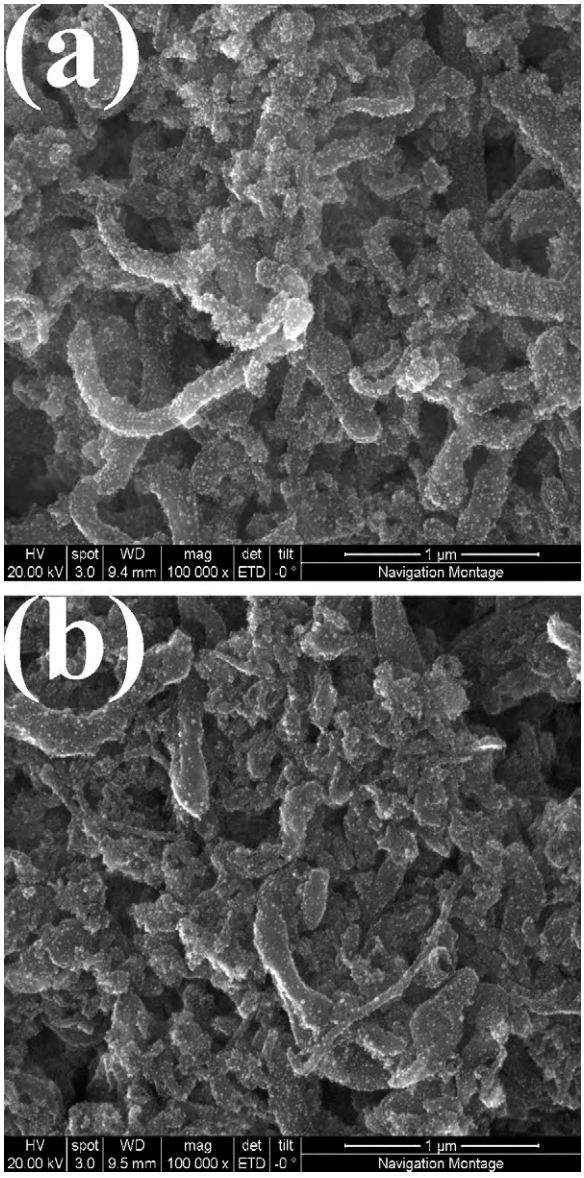

Fig. 1. FESEM images of Pd/CNFs-E (a) and Pd/CNFs-C (b).

3. Results and discussion

3.1. FESEM, HRTEM and XRD characterization

Fig. 1(a) and (b) shows the FESEM images of Pd nanoparticles deposited on CNFs by electrochemical and chemical reduction methods, respectively. It can be seen that the Pd nanoparticles synthesized by either method are well dispersed on CNFs and the particles synthesized by electrochemical method (PED) display a higher distribution density, which is attributed to the higher ratio

of Pd particles to available CNFs in Pd/CNFs/GC-E electrode. In the Pd/CNFs/GC-C electrode, all the CNFs are well decorated by Pd particles. While in the Pd/CNFs/GC-E electrode, only the CNFs accessible to Pd plating bath can be decorated with Pd particles. Therefore the Pd particles in the Pd/CNFs/GC-E electrode have a higher distribution density. Although the CNFs are not all accessible to Pd particles in Pd/CNFs/GC-E electrode, the CNFs supported Pd particles in the electrode are all accessible to reactants. On the contrary, although the CNFs are all accessible to Pd particles in Pd/CNFs/GC-C electrode, the CNFs supported Pd particles are not all accessible to reactants. It is worth noting that the film of Pd/CNFs-E is more porous than that of Pd/CNFs-C, so the Pd particles in the Pd/CNFs/GC-E electrode can be more accessible to reactants, leading to a higher utilization of Pd catalyst in Pd/CNFs/GC-E electrode.

The HRTEM images of Pd particles deposited on CNFs by electrochemical and chemical methods are shown in Fig. 2(a) and (b), respectively. It can be seen that Pd particles synthesized by either method are uniformly dispersed on CNFs and the Pd particles synthesized by PED have a slightly larger average particle size (as seen from Fig. 2(c) and (d)). It is believed that the surface functional groups on the CNFs are main anchoring sites for noble metal particles [16], so the uniform dispersion of Pd nanoparticles indicates that sonochemical treatment is an effective method to uniformly import oxygen-containing groups onto CNFs. The relatively strong metal-support interaction between Pd particles and CNFs may also contribute to the good dispersion [19].

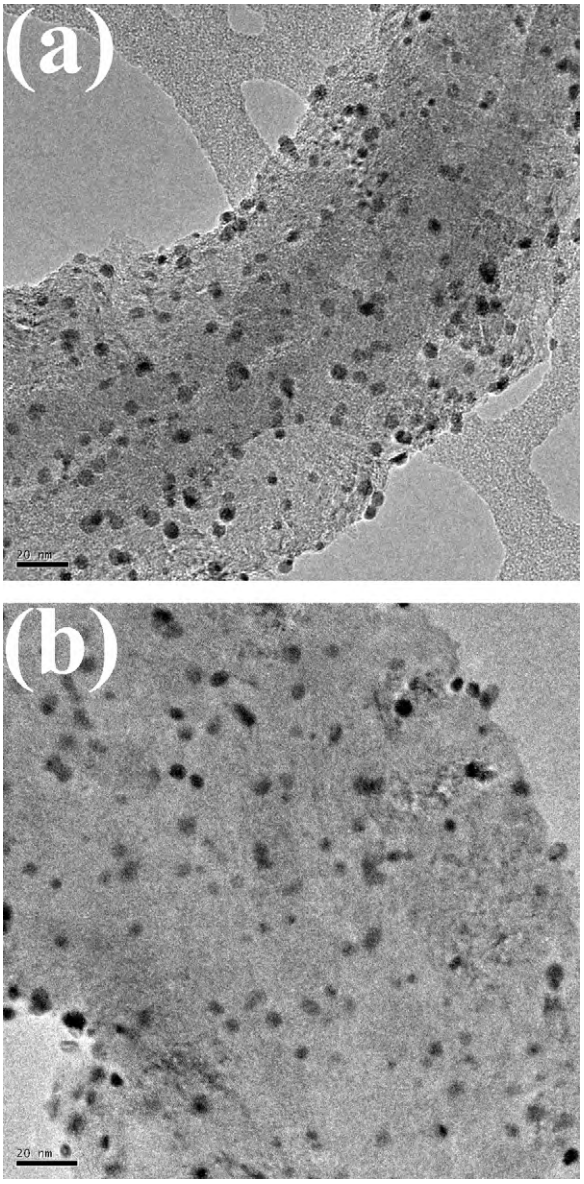

Fig. 2. HRTEM images of Pd/CNFs-E (a) and Pd/CNFs-C (b); the size distribution of Pd particles on Pd/CNFs-E (c) and Pd/CNFs-C (d).

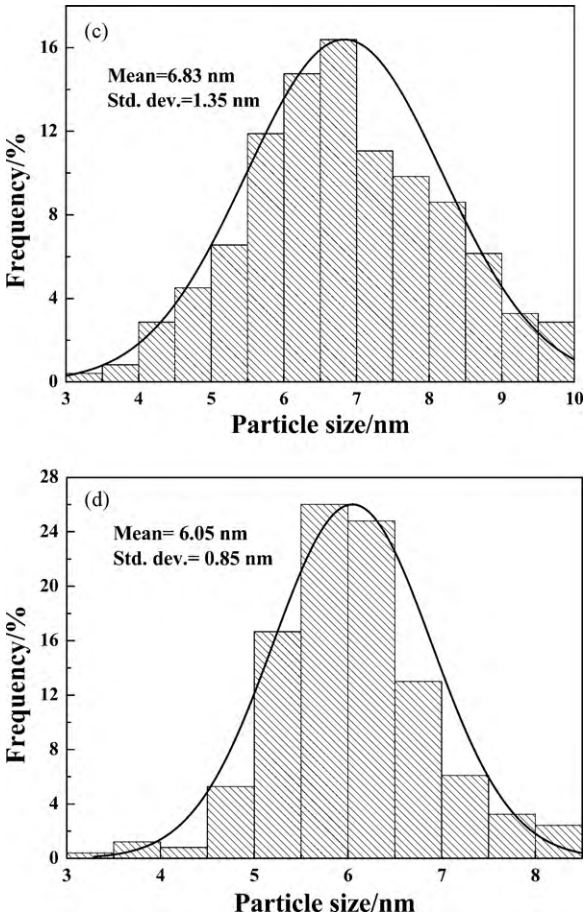

Fig. 2. (*Continued*).

The XRD patterns of the Pd/CNFs-C (a) and Pd/CNFs-E (b) catalysts are shown in Fig. 3. The main diffraction peaks of Pd nanoparticles can be observed on both the XRD patterns of

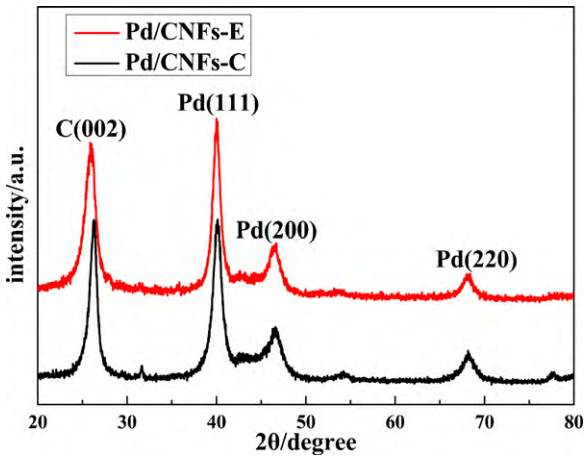

Fig. 3. XRD patterns of Pd/CNFs-E and Pd/CNFs-C catalysts.

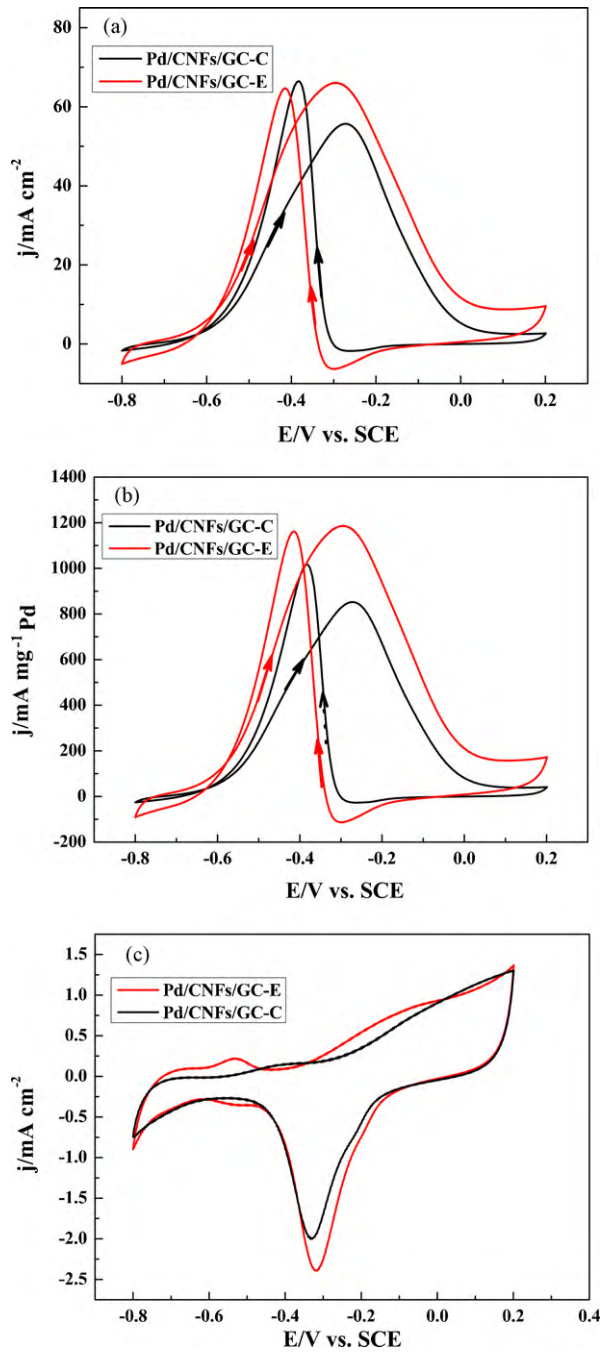

Fig. 4. Cyclic voltammograms for Pd/CNFs/GC-E and Pd/CNFs/GC-C in 1 M KOH with (a), (b) and without (c) 1 M ethanol solution with a scanning rate of 50 mV s^{-1} at room temperature.

Pd/CNFs-C (a) and Pd/CNFs-E (b) catalysts, and all peaks can be indexed as Pd cubic crystallite. The Pd (2 0 0) peak was used to calculate the particle size of Pd according to the Scherrer formula and the particle size of Pd was found to be 6.1 and 6.9 nm in the case of Pd/CNFs-C and Pd/CNFs-E catalysts, respectively, which is consistent with the HRTEM results.

3.2. Cyclic voltammetry (CV)

Fig. 4(a) represents the cyclic voltammograms of Pd/CNFs/GC-E and Pd/CNFs/GC-C electrodes in deaerated 1 M KOH + 1 M ethanol with a scanning rate of 50 mV s^{-1} in the potential range from −0.8 to 0.2 V at room temperature. The onset potential for ethanol oxidation is at −0.751 V for Pd/CNFs/GC-E electrode while at −0.734 V for Pd/CNFs/GC-C electrode. The peak current density on the forward scan is 66.1 mA cm^{-2} (peak potential at −0.297 V) for Pd/CNFs/GC-E electrode and 54.9 mA cm^{-2} (peak potential at −0.273 V) for Pd/CNFs/GC-C electrode. It can be clearly seen that the EOR at Pd/CNFs/GC-C electrode has positive onset and peak potentials, which suggests that the ethanol oxidation kinetics on the Pd/CNFs/GC-C electrode is more sluggish than that on the Pd/CNFs/GC-E electrode. Two well-defined oxidation peaks can be clearly observed from the CV curves. The oxidation peaks on the forward scan is corresponding to the oxidation of freshly chemisorbed species coming from ethanol adsorption, while the reverse scan peak is primarily associated with removal of carbonaceous species not completely oxidized in the forward scan [17,20]. So the ratio of the forward anodic peak current density (j_f) to the reverse anodic peak current density (j_b), j_f/j_b, could be used as a criterion to evaluate contamination arisen from the poisoning species [21]. A low j_f/j_b ratio indicates poor oxidation of ethanol to carbon dioxide during the anodic scan and excessive accumulation of carbonaceous residues on electrode surface [22]. Obviously, the j_f/j_b ratio in Pd/CNFs/GC-E electrode is larger than unity, while the ratio in Pd/CNFs/GC-C electrode is smaller than unity. This implies that the Pd/CNFs/GC-E electrode has a better tolerance to poisoning than the Pd/CNFs/GC-C electrode.

Obviously, the electrocatalytic activity of Pd/CNFs/GC-E electrode is better than that of Pd/CNFs/GC-C electrode. The mass activity is 1187 and 852 mA mg_{Pd}^{-1} in the case of Pd/CNFs/GC-E and Pd/CNFs/GC-C electrode, respectively (as shown in Fig. 4(b)). It is worth noting that the average Pd particle size of Pd/CNFs/GC-E is larger than that of Pd/CNFs/GC-C electrode. So the nearly 40% increase in the mass activity of Pd/CNFs/GC-E electrode relative to that of Pd/CNFs/GC-C electrode is most likely due to the higher utilization of Pd catalyst on the former electrode.

To estimate the utilization of Pd catalyst, the electrochemically active surface areas (EASA) of the two electrodes were evaluated by determining the coulombic charge for the reduction of Pd oxide. As shown in Fig. 4(c), the Pd oxide reduction peak appears at ca. −0.320 V on the cyclic voltammograms in the deaerated 1 M KOH solution. The coulombic charge for the reduction of Pd oxide was determined by integrating the oxide reduction peak. The EASA based on the coulombic charge are 7.95 and 6.72 mC cm^{-2} for Pd/CNFs/GC-E and Pd/CNFs/GC-C, respectively. If the utilization of Pd catalyst on the Pd/CNFs/GC-C electrode is the same as that on the Pd/CNFs/GC-E electrode, the former with a higher Pd loading and relatively small Pd particle size will have a larger EASA. So the relatively small EASA demonstrated by the Pd/CNFs/GC-C electrode confirms that the available Pd active sites on it are lower than that on the Pd/CNFs/GC-E electrode. As mentioned above, the powder type electrode fabrication method used in the present study tends to decrease the utilization of Pd catalyst because ethanol solution may have difficulty in accessing the inner electrocatalytic sites of the Pd/CNFs/GC-C electrode. In addition, the necessary addition of Nafion tends to isolate some Pd nanoparticles from CNFs, leading to a poor electron transport [10] and low utilization of Pd catalyst. While in the electrode fabricated by PED method, all the Pd particles were selectively deposited on the sites that can be accessed by the Pd plating solution, so the Pd deposited sites certainly can be accessed by ethanol solution, resulting in a high utilization of Pd catalyst. In addition, the selective electrodeposition of Pd on the CNFs promises to improve the Pd utilization by securing the electronic route from Pd to the supporting electrode. It is interesting to note that the peak currents per coulombic charge for the reduction of Pd oxide are almost the same (8.3 A C^{-1} for Pd/CNFs/GC-E and 8.2 A C^{-1} for Pd/CNFs/GC-C), which confirms our speculation that the differences in electrocatalytic activities are primarily a result of the different utilization of Pd catalyst on the two electrodes.

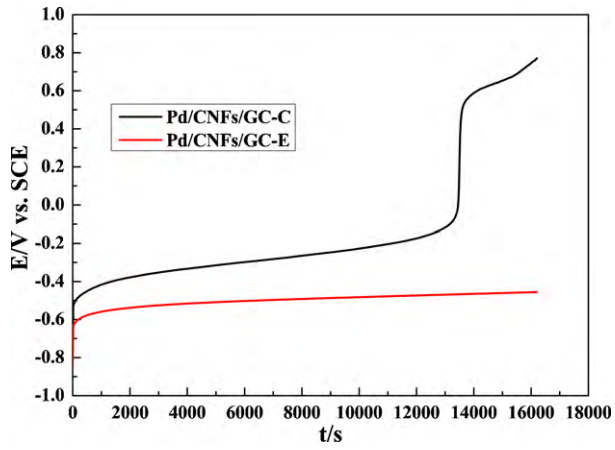

Fig. 5. Chronopotentiometric curves of ethanol oxidation on the two electrodes at 3 mA cm^{-2} in 1 M KOH + 1 M ethanol solution.

3.3. Chronopotentiometry (CP)

CP was employed to check the stability of Pd/CNFs/GC electrodes for ethanol oxidation at room temperature. Fig. 5 represents the respective CP curves for ethanol oxidation on Pd/CNFs/GC-E and Pd/CNFs/GC-C at 3 mA cm^{-2}. The oxidation of ethanol on Pd/CNFs/GC-E electrode was relatively stable. However, on the Pd/CNFs/GC-C electrode, the ethanol oxidation potential gradually increased and finally shifted to a higher value for oxygen evolution instead of the ethanol oxidation [23]. The CP results are consistent with the above CV results, and both indicate that the Pd/CNFs/GC-E electrode has a better stability than Pd/CNFs/GC-C electrode. This may be because compare with the Pd nanoparticles deposited by chemical method, the Pd nanoparticles deposited by electrochemical method adopted a more preferred crystallographic orientation as a result of the stronger interaction between electrodeposited Pd particles and CNFs, leading to a better poisoning tolerance of Pd/CNFs/GC-E electrode relative to Pd/CNFs/GC-C electrode.

4. Conclusions

Using EPD in conjunction with PED technique, the novel Pd/CNFs/GC-E electrode was fabricated and its performance was compared with the Pd/CNFs/GC-C electrode fabricated by the conventional powder type technique. Although the Pd loading on the Pd/CNFs/GC-E electrode is lower than that on the Pd/CNFs/GC-C electrode and the Pd particle size of the former is slightly larger than that of the latter, the former exhibits a higher electrocatalytic activity for ethanol oxidation as compared with the latter. This is believed to be due to the higher available Pd active sites on the Pd/CNFs/GC-E electrode than on the Pd/CNFs/GC-C electrode. The results demonstrate the electrode fabrication methods have a significant influence on the performance of the prepared electrodes, and the non-powder type electrode fabrication method has great potential for fabricating electrodes with high utilization of noble metals.

Acknowledgements

The present study was supported by the open foundation of the State Key Laboratory of Electroanalytical Chemistry (Changchun Institute of Applied Chemistry, Chinese Academy of Sciences), Shanghai Key Laboratory of Green Chemistry and Chemical Process (East China Normal University) and the State Key Laboratory Breeding Base of Green Chemistry Synthesis Technology (Zhejiang University of Technology).

References

[1] C. Lamy, A. Lima, V. LeRhun, F. Delime, C. Coutanceau, J. Léger, J. Power Sources 105 (2002) 283–296.
[2] C. Xu, P. Shen, X. Ji, R. Zeng, Y. Liu, Electrochem. Commun. 7 (2005) 1305–1308.
[3] E. Antolini, J. Power Sources 170 (2007) 1–12.
[4] P. Shen, C. Xu, Electrochem. Commun. 8 (2006) 184–188.
[5] C. Bianchini, P. Shen, Chem. Rev. 109 (2009) 4183–4206.
[6] G. Girishkumar, K. Vinodgopal, P.V. Kamat, J. Phys. Chem. B 108 (2004) 19960–19966.
[7] J.-S. Zheng, X.-S. Zhang, P. Li, J. Zhu, X.-G. Zhou, W.-K. Yuan, Electrochem. Commun. 9 (2007) 895–900.
[8] F. Alcaide, G. Álvarez, O. Miguel, M.J. Lázaro, R. Moliner, A. López-Cudero, J. Solla-Gullón, E. Herrero, A. Aldaz, Electrochem. Commun. 11 (2009) 1081–1084.
[9] T. Maiyalagan, Int. J. Hydrogen Energy 34 (2009) 2874–2879.
[10] C. Wang, M. Waje, X. Wang, J. Tang, R. Haddon, Y. Yan, Nano Lett. 4 (2004) 345–348.
[11] K. Choi, H. Kim, T. Lee, J. Power Sources 75 (1998) 230–235.
[12] H. Kim, N.P. Subramanian, B.N. Popov, J. Power Sources 138 (2004) 14–24.
[13] G. Girishkumar, M. Rettker, R. Underhile, D. Binz, K. Vinodgopal, P. McGinn, P. Kamat, Langmuir 21 (2005) 8487–8494.
[14] T. Zhao, Y. Zhu, P. Li, D. Chen, Y. Dai, W. Yuan, A. Holmen, Chin. J. Catal. 25 (2004) 829–833.
[15] J.-H. Zhou, Z.-J. Sui, P. Li, D. Chen, Y.-C. Dai, W.-K. Yuan, Carbon 44 (2006) 3255–3262.
[16] Y. Xing, J. Phys. Chem. B 108 (2004) 19255–19259.
[17] R.N. Singh, A. Singh, Anindita, Carbon 47 (2009) 271–278.
[18] L. Jiang, L. Gao, J. Sun, J. Colloid Interface Sci. 260 (2003) 89–94.
[19] C. Pham-Huu, N. Keller, G. Ehret, L. Charbonniere, R. Ziessel, M. Ledoux, J. Mol. Catal. A – Chem. 170 (2001) 155–163.
[20] J. Liu, J. Ye, C. Xu, S.P. Jiang, Y. Tong, Electrochem. Commun. 9 (2007) 2334–2339.
[21] G.-Y. Zhao, C.-L. Xu, D.-J. Guo, H. Li, H.-L. Li, J. Power Sources 162 (2006) 492–496.
[22] T. Huang, R. Jiang, D. Zhang, J. Zhuang, W. Cai, A. Yu, J. Solid State Electr. 14 (2010) 101–107.
[23] F. Hu, F. Ding, S. Song, P. Shen, J. Power Sources 163 (2006) 415–419.